JOURNAL OF CHEMICAL & ENGINEERING DATA

ARTICLE

pubs.acs.org/jced

Adsorption Equilibrium of Water Vapor on Selexsorb-CDX Commercial Activated Alumina Adsorbent

Atanas Serbezov,* Joshua D. Moore,† and Yaqin Wu‡

Department of Chemical Engineering, Rose-Hulman Institute of Technology, 5500 Wabash Avenue, CM 49, Terre Haute, Indiana 47803, United States

ABSTRACT: Adsorption equilibrium data of water vapor on a commercially available activated alumina, Selexsorb-CDX, were measured by a static gravimetric technique. The relative humidity and temperature were varied between 0 % and 90 % and between (5 and 35) °C, respectively. The measured data were fitted to the dual mechanism adsorption potential (DMAP) equation. The pore structure of the adsorbent material was characterized by nitrogen adsorption and mercury intrusion measurements. The DMAP equation predicted that the first 50 % of the total water adsorbed was held on the adsorbent by the combined action of chemisorption and physisorption, which was attributed to filling of the micropores and the first adsorbed layers in the mesopores. The remainder of the adsorbed water was attributed to capillary condensation in the mesopores. The heat of adsorption as a function of fractional loading was calculated using the fitted DMAP equation parameters in conjunction with the van't Hoff equation, with and without an assumption of the Clausius−Clapeyron equation. The two methods for the heat of adsorption calculation were in excellent agreement, differing by no more than 0.2 $kJ \cdot mol^{-1}$. The reported experimental data and correlation parameters can be readily applied in the modeling, design, and optimization of dehumidification processes utilizing the Selexsorb-CDX activated alumina adsorbent used in this study.

INTRODUCTION

Activated alumina adsorbents are widely used as desiccants in both heated (temperature swing adsorption) and heatless (pressure swing adsorption) dryers. They exhibit a large surface area and high strength against crushing and stable physical and chemical characteristics, even in high temperature and corrosive environments. In addition, they are resistant to thermal shock and do not shrink, swell, soften, or disintegrate when immersed in water.[1]

Commercial production of activated alumina is performed by thermal dehydration or activation of aluminum trihydrate ($Al(OH)_3$, or $Al_2O_3 \cdot 3H_2O$).[2] During the manufacturing process, the initial material undergoes complex phase transformations that depend on the heat treatment conditions.[2] Activated alumina manufacturers employ proprietary activation processes to tailor the adsorption properties of their activated alumina products. In many cases additives, such as alkali metal salts,[1] are also used to achieve improved performance characteristics. As a result of the significant number of controlled variations in the manufacturing process, there are many types of activated alumina available commercially. The selection of a specific activated alumina for a specific application requires knowledge and understanding of its adsorption properties.

Despite the practical importance of activated alumina in desiccant applications and the wide variety of commercially available activated alumina adsorbents, there are relatively few adsorption equilibrium data sets available in the literature for the activated alumina/water vapor system. Adsorption isotherms for water vapor on nine different activated alumina adsorbents manufactured by Rhone-Poulenc, Alcan, and Alcoa were determined by Desai et al.[3] by both gravimetric and dynamic methods. Kotoh et al.[4] obtained data on activated alumina made by Nakarai Chemicals, Ltd. using a dynamic gravimetric setup. Kim et al.[5] reported data measured by a static volumetric method for an activated alumina adsorbent supplied by Procatalyze Co. Serbezov[6] used a static gravimetric technique to obtain data for F-200 manufactured by Alcoa. Data for F-200 were also reported by Li et al.[7] who used a hybrid gravimetric/volumetric technique. Ribeiro et al.[8] used a gravimetric technique to obtain data on basic activated alumina supplied by Norton.

The present study focuses on the desiccant properties of a commercially available activated alumina material with a trade name Selexsorb-CDX. We quantify its ability to retain water vapor by measuring adsorption isotherms at four different temperatures using a static gravimetric technique. The obtained adsorption isotherm data are fitted to the dual mechanism adsorption potential (DMAP) model developed previously by Moore and Serbezov[9] from a methodology first proposed by Kotoh et al.[4] We characterize the pore structure of the adsorbent material using nitrogen adsorption and mercury intrusion measurements. We analyze the fitted DMAP model parameters together with the pore size characterization results to gain insights into the mechanisms by which water is retained on the adsorbent. Finally, we calculate the isosteric heat of adsorption using the van't Hoff equation in conjunction with the DMAP model parameters, with and without an assumption of the Clausius−Clapeyron equation.

EXPERIMENTAL SECTION

Materials. The Selexsorb-CDX activated alumina adsorbent was manufactured by Alcoa. (The adsorbents division of Alcoa is now part of BASF Catalysts LLC.) For simplicity, we will refer to

Received: May 5, 2010
Accepted: April 15, 2011
Published: April 28, 2011

dx.doi.org/10.1021/je100473f | J. Chem. Eng. Data 2011, 56, 1762–1769

the material simply as CDX. The water used in the adsorption experiments was high purity HPLC grade.

Material Characterization. Nitrogen (N_2) adsorption and desorption isotherms were measured at 77.35 K using an Autosorb iQ gas sorption analyzer. Mercury (Hg) intrusion measurements were performed with a PoreMaster 60 porosimeter capable of generating pressures up to 60 000 psia. Both instruments are manufactured by Quantachrome Instruments (Boynton Beach, FL). The material characterization measurements were performed by Quantachrome's Material Characterization Laboratory (LabQMC).

Adsorption Isotherm Measurements. The adsorption equilibrium data reported in this study were obtained by a static gravimetric technique. The adsorption equipment was an IGA-002 (Intelligent Gravimetric Analyzer) system manufactured by Hiden Analytical, Ltd. (U.K.). This is a fully automated apparatus designed for gravimetric measurements of adsorption and desorption. The microbalance has a sample capacity of 200 mg and a weighing resolution of 0.1 μg. The temperature in the vicinity of the sample was measured by a platinum resistance thermometer with a precision of $\pm$ 0.1 °C. The pressure was measured by a capacitance manometer with a range of 100 mbar and a precision of $\pm$ 0.02 mbar. The experimental setup and procedure are briefly summarized below and described in detail in an earlier publication by Serbezov.[6]

A small amount of adsorbent, (85 to 100) mg dry mass, was placed into a sample holder and regenerated at 290 °C under vacuum (10^{-6} mbar) for 48 h. Upon regeneration, the desired isotherm temperature was set and maintained in the adsorption vessel. The pressure was then increased in step increments until the highest pressure on the isotherm was reached and then decreased in the same manner back to vacuum conditions. Each pressure level was maintained for 10 h. The mass of the sample was constantly monitored and recorded. We have observed that, in all cases, the sample mass had reached a constant value at the end of each 10 h period, which was recorded as the equilibrium mass at the given conditions. Upon completion of the adsorption/desorption sequence, the sample was regenerated and used for another adsorption/desorption experiment at a different (or the same) temperature.

THEORY

The experimental adsorption equilibrium data reported in this study were correlated using the DMAP equation developed by Moore and Serbezov[9] following a methodology first proposed by Kotoh et al.[4] The form of the DMAP equation is

$$q = q_{s1}\left(\frac{P}{P_o(T)}\right)^{R_gT/E_1} + (q_{s2} - q_{s1})\left(\frac{P}{P_o(T)}\right)^{R_gT/E_2} \quad (1)$$

In eq 1 q is the equilibrium molar loading of water vapor at the equilibrium water vapor pressure P, $P_o(T)$ is the water vapor saturation pressure at temperature T, R_g is the ideal gas law constant, T is the absolute temperature, and E_1 and E_2 are characteristic energies of adsorption. The parameter q_{s1} is the maximum molar loading of water vapor due to the combined contribution of chemisorption and physisorption. The parameter q_{s2} is the maximum total molar loading of water vapor due to all mechanisms, that is, chemisorption, physisorption, and capillary condensation. The difference $(q_{s2} - q_{s1})$ is the maximum molar loading due to capillary condensation alone.

The first term in eq 1 accounts for the combined effect of chemisorption and physisorption, while the second term accounts for capillary condensation. We have combined the chemisorption and physisorption mechanisms because, in our experimental setup, we can only measure the combined effect of the two mechanisms. This is explained in greater detail by Moore and Serbezov.[9]

The DMAP equation has three fitting parameters: q_{s1}, E_1, and E_2. The fourth parameter q_{s2} is calculated from the total pore volume of the adsorbent, V_m, which can be measured independently and is typically reported by the adsorbent manufacturers.

$$q_{s2} = \frac{V_m\rho}{MW} \quad (2)$$

In eq 2 ρ and MW are the liquid density and the molecular weight of water, respectively. The DMAP equation can be rewritten in terms of the adsorption potential,[9] A

$$q = q_{s1}\exp\left(-\frac{A}{E_1}\right) + (q_{s2} - q_{s1})\exp\left(-\frac{A}{E_2}\right) \quad (3)$$

The adsorption potential is given by the expression[10]

$$A = R_gT\ln\left(\frac{P_o(T)}{P}\right) \quad (4)$$

The benefit of using the adsorption potential form of the DMAP equation, eq 3, is that data obtained at different temperatures are fitted by a single curve. This significantly simplifies the correlation procedure, and one set of fitted parameters can be used over a range of temperatures.

The heat of adsorption, $-\Delta H(T)$, at a given temperature, T, is commonly defined through the van't Hoff equation:[10]

$$-\Delta H(T) = R_gT^2\left(\frac{\partial \ln P}{\partial T}\right)_q = -R_g\left(\frac{\partial \ln P}{\partial(1/T)}\right)_q \quad (5)$$

The partial derivative on the right-hand side of eq 5 can be calculated from the slopes of the isosteres, that is, $(\ln P)$ vs $(1/T)$ at constant loading,[11] which are generally linear over moderate temperature ranges.

Moore and Serbezov[9] showed that the van't Hoff equation can be significantly simplified if the following two conditions are valid:

- The Clausius−Clapeyron[12] equation applies to describe the change in vapor pressure with respect to temperature, that is, $d\ln P_o(T)/dT = \Delta H_{vap}(T)/(R_gT^2)$, where $\Delta H_{vap}(T)$ is the heat of vaporization at temperature, T.
- The adsorption equilibrium is well-described by the DMAP equation.

With these two assumptions, the resulting equation for the heat of adsorption is[9]

$$-\Delta H(T) = \Delta H_{vap}(T) + A = \Delta H_{vap}(T) + R_gT\ln\left(\frac{P_o(T)}{P}\right) \quad (6)$$

Equation 6 provides a much easier way of calculating the heat of adsorption, $-\Delta H(T)$, as long as the above two conditions are met, since it does not depend on any of the fitted DMAP parameters. Although the heat of adsorption, $-\Delta H(T)$, in eq 6 is not an explicit function of the equilibrium molar loading, q, it can be related to q numerically through the DMAP equation. To construct a plot of $-\Delta H(T)$ versus q using eqs 6 and 1, both

Table 1. Physical Properties of Selexsorb-CDX Activated Alumina

property	determined in this study		listed by the manufacturer (methods not reported)
	value	method	
form	spherical	visual inspection	spherical
diameter/mm	NA		3.2
total pore volume/$cm^3 \cdot g^{-1}$	0.514	N_2 adsorption at $P/P_o = 1$	0.5
micropore volume/$cm^3 \cdot g^{-1}$ (pore diameter < 20 Å)	0.118	*t*-plot, de Boer equation	NA
macropore volume/$cm^3 \cdot g^{-1}$ (pore diameter > 500 Å)	0.088	Hg intrusion, Washburn equation	NA
surface area/$m^2 \cdot g^{-1}$	469	single-point BET $P/P_o = 0.3$	450
	458	multipoint BET $P/P_o = 0.05$ to 0.3	
	521	multipoint BET $P/P_o = 0.01$ to 0.05	
packed bulk density/$kg \cdot m^{-3}$	NA		665

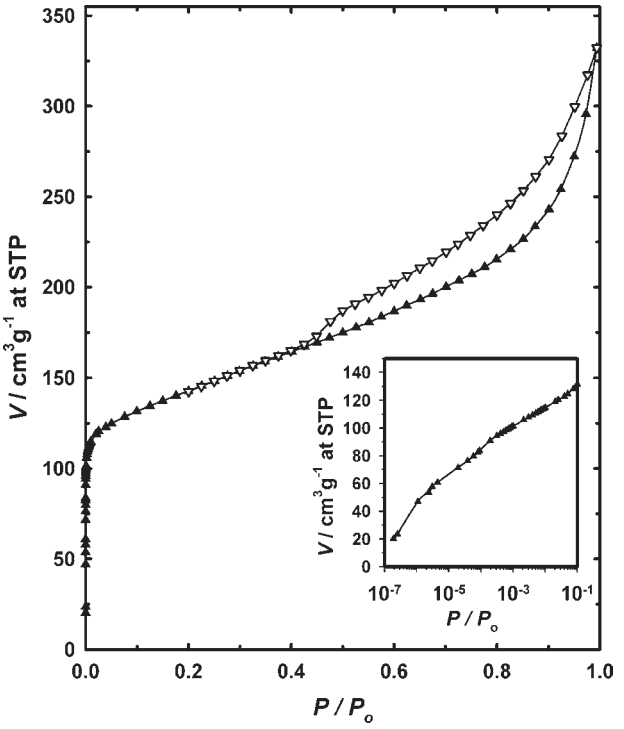

Figure 1. Adsorbed (▲)and desorbed (▽) STP volumes, *V*, of N_2 on Selexsorb-CDX at 77.35 K as a function of N_2 relative pressure, P/P_o. STP conditions are 1.01325 bar and 273.15 K. P_o is the N_2 vapor pressure at 77.35 K. Low pressure adsorption is shown as an insert with the relative pressure on a log scale. Lines are drawn as a guide for the eye.

equations are solved over a range of partial pressures, and the obtained $-\Delta H(T)$ and q values are plotted against each other.

RESULTS AND DISCUSSION

Adsorbent Characterization Using N_2 Adsorption and Hg Intrusion. The adsorbent material (Selexsorb-CDX) has been characterized by N_2 adsorption at 77.35 K and Hg intrusion. The results from the characterization studies are summarized in Table 1. The N_2 adsorption and desorption isotherms at 77.35 K are shown in Figure 1 as a function of the relative N_2 pressure, P/P_0. Referring to the IUPAC classification,[13] the N_2 adsorption/desorption isotherm of CDX at 77.35 K most closely resembles a type IV isotherm with type H3 hysteresis, which is normally indicative of a mesoporous material without micropores.[13] However, from Figure 1 we observe a significant increase of adsorbed N_2 in the very low range of relative pressures, $P/P_o \ll 0.01$, which suggests the presence of micropores (pore diameter < 20 Å). A *t*-plot[10] was used to confirm microporosity, with the total micropore volume estimated as 0.118 $cm^3 \cdot g^{-1}$ for pores < 20 Å based on the de Boer equation.[14]

At pressures near saturation, $P/P_o \approx 1$, the N_2 adsorption/desorption isotherm does not level off, suggesting the presence of macropores (pore diameter > 500 Å). The macroporosity was confirmed using Hg intrusion, with a total macropore volume estimated as 0.088 $cm^3 \cdot g^{-1}$ for pores > 500 Å based upon the Washburn equation.[15]

The total pore volume of CDX has been estimated from the N_2 adsorption isotherm at $P/P_o = 1$. The measured value of 0.514 $cm^3 \cdot g^{-1}$ agrees well with the value reported by the manufacturer as a multiple lot average for the CDX material (0.5 $cm^3 \cdot g^{-1}$).

The surface area of CDX has been estimated by applying the Brunauer–Emmett–Teller (BET) equation[16] to two different relative pressure ranges in the N_2 adsorption isotherm. When the BET equation is applied in the standard[17] range $P/P_o = 0.05$ to 0.3, a value similar to the one reported by the manufacturer is obtained. However, recently it has been shown that for microporous materials, more accurate surface area estimates are obtained when the BET equation is applied using a consistency criterion.[17] The consistency criterion for our data leads to the range $P/P_o = 0.01$ to 0.05. The multipoint BET surface area calculated for $P/P_o = 0.01$ to 0.05 is 521 $m^2 \cdot g^{-1}$ compared to 458 $m^2 \cdot g^{-1}$ for $P/P_o = 0.05$ to 0.3.

Water Vapor Adsorption on Selexsorb-CDX. Adsorption isotherms for water vapor on CDX were measured at (5, 15, 25, and 35) °C in the range of 0 % to approximately 90 % relative humidity. The adsorption isotherm data are presented in Tables 2 to 5. Multiple measurements at the same experimental conditions enabled the estimation of the experimental uncertainty associated with the data. We summarize the experimental uncertainty (95 % confidence) in Table 6 at the conditions for which three or more replicate measurements are available. The experimental uncertainty (δ) is estimated using the expression[18]

$$\delta = t_{\alpha/2}\frac{S}{\sqrt{n}} \tag{7}$$

where n is the number of replicate measurements, S is the standard deviation of the replicate measurements, and $t_{\alpha/2}$ is

Table 2. Isotherm Data at 5 °C

t = 5 °C		P_o(5 °C) = 8.706 mbar	
adsorption			
P/mbar	P/P_0	q/mmol·g^{-1}	A/kJ·mol^{-1}
0.50	0.0574	8.0780	6.607
0.50	0.0574	7.9925	6.607
0.50	0.0574	7.9523	6.607
1.49	0.1711	9.2682	4.082
1.49	0.1711	9.2035	4.082
1.50	0.1723	9.5048	4.067
2.09	0.2401	9.7947	3.300
2.09	0.2401	9.7202	3.300
2.12	0.2435	10.0103	3.267
3.29	0.3779	10.9131	2.250
3.30	0.3790	11.1777	2.243
3.30	0.3790	10.8226	2.243
4.99	0.5732	12.9337	1.287
4.99	0.5732	12.8301	1.287
5.00	0.5743	13.2389	1.282
5.79	0.6651	14.3434	0.943
5.79	0.6651	14.1995	0.943
5.80	0.6662	14.0674	0.939
7.50	0.8615	17.4579	0.345
7.50	0.8615	17.2471	0.345
7.50	0.8615	17.5816	0.345
desorption			
P/mbar	P/P_0	q/mmol·g^{-1}	A/kJ·mol^{-1}
5.79	0.6651	15.8656	0.943
5.79	0.6651	15.5524	0.943
5.79	0.6651	15.4643	0.943
5.00	0.5743	14.7545	1.282
5.00	0.5743	14.3041	1.282
5.00	0.5743	14.2696	1.282
4.99	0.5732	14.1561	1.287
4.99	0.5732	14.1836	1.287
3.30	0.3790	11.7573	2.243

Table 3. Isotherm Data at 15 °C

t = 15 °C		P_o(15 °C) = 17.081 mbar	
adsorption			
P/mbar	P/P_0	q/mmol·g^{-1}	A/kJ·mol^{-1}
0.99	0.0580	8.0791	6.823
1.00	0.0585	8.1074	6.799
1.00	0.0585	8.0621	6.799
1.48	0.0866	7.9007	5.860
2.00	0.1171	8.5705	5.138
2.00	0.1171	8.9435	5.138
2.00	0.1171	8.8775	5.138
2.00	0.1171	8.8503	5.138
5.99	0.3507	11.0012	2.510
5.99	0.3507	10.8814	2.510
6.00	0.3513	11.2444	2.506
6.00	0.3513	10.8101	2.506
7.99	0.4678	12.0878	1.820
8.00	0.4684	12.2579	1.817
8.00	0.4684	12.4983	1.817
8.00	0.4684	11.9892	1.817
11.99	0.7019	15.2700	0.848
11.99	0.7019	15.3377	0.848
12.00	0.7025	15.6069	0.846
12.00	0.7025	15.1866	0.846
14.99	0.8776	18.5898	0.313
15.00	0.8782	19.0028	0.311
15.01	0.8788	19.1469	0.310
15.02	0.8793	18.9408	0.308
desorption			
P/mbar	P/P_0	q/mmol·g^{-1}	A/kJ·mol^{-1}
14.00	0.8196	18.9291	0.477
11.99	0.7019	17.5166	0.848
11.99	0.7019	17.0194	0.848
8.00	0.4684	14.1448	1.817
8.00	0.4684	13.6819	1.817
6.00	0.3513	11.6095	2.506
6.00	0.3513	11.7002	2.506
2.00	0.1171	9.5021	5.138
1.00	0.0585	8.8971	6.799
1.00	0.0585	8.6738	6.799

the Student's t distribution calculated at $(n - 1)$ degrees of freedom and a confidence level $(\alpha/2)$. In Table 6, $\alpha = 0.05$ which corresponds to a 95 % confidence interval.

The ratio of the experimental uncertainty and the average loading, $\delta/\bar{q}$, reported in Table 6 represents the relative uncertainty. The relative uncertainty values for the experimental measurements listed in Table 6 are less than 5 % with the majority of them falling in the range from 2 % to 3 %.

Plots of equilibrium loading versus adsorption potential are shown in Figure 2. Also shown in Figure 2 are the DMAP equation fits of the experimental data. The fits are obtained with a nonlinear regression routine based on the Marquardt—Levenberg algorithm and implemented in the SigmaPlot computer program.[19]

The best-fit values of the DMAP equation regression parameters and their standard errors are listed in Table 7. The standard errors quantify the precision of the best-fit values and can be used to compute confidence intervals. For all parameters listed in Table 7, the 95 % confidence interval is centered at the best-fit value and extends approximately two standard errors on both sides (above and below).

Table 8 presents a summary of the statistical measures associated with the DMAP equation fits. The coefficient of determination (R^2) describes how close the fitted curve comes to the data. The R^2 values are high for both adsorption and desorption, indicating that the DMAP equation fits the data well. The standard error of estimate (SEE) quantifies the uncertainty in the regression curve, and it is much smaller for the adsorption data compared to the desorption data. The Durbin-Watson (D-W) statistic is a measure of the correlation between the residuals (i.e., the difference between the observed and predicted

dx.doi.org/10.1021/je100473f |J. Chem. Eng. Data 2011, 56, 1762–1769

Table 4. Isotherm Data at 25 °C

t = 25 °C		P_o(25 °C) = 31.788 mbar	
adsorption			
P/mbar	P/P_0	q/mmol·g^{-1}	A/kJ·mol^{-1}
0.99	0.0311	7.5757	8.599
1.00	0.0315	7.3268	8.574
2.50	0.0786	8.4408	6.303
2.50	0.0786	8.6253	6.303
4.49	0.1412	9.2354	4.852
4.49	0.1412	9.3737	4.852
6.99	0.2199	10.0828	3.754
7.00	0.2202	9.9740	3.751
9.99	0.3143	10.8102	2.869
9.99	0.3143	10.8806	2.869
15.99	0.5030	12.8109	1.703
15.99	0.5030	12.8103	1.703
19.99	0.6289	14.4623	1.150
20.00	0.6292	14.5184	1.149
25.00	0.7865	17.3941	0.595
25.02	0.7871	17.2698	0.593
27.99	0.8805	19.8775	0.315
27.99	0.8805	20.1711	0.315
desorption			
P/mbar	P/P_0	q/mmol·g^{-1}	A/kJ·mol^{-1}
25.01	0.7868	18.4452	0.594
25.00	0.7865	18.6577	0.595
20.00	0.6292	16.3174	1.149
16.00	0.5033	14.2599	1.702
9.99	0.3143	11.6894	2.869
9.99	0.3143	11.6887	2.869
7.00	0.2202	10.7616	3.751
6.99	0.2199	10.7114	3.754
4.50	0.1416	10.1022	4.846
2.50	0.0786	9.2943	6.303
2.50	0.0786	9.4245	6.303
1.00	0.0315	8.4439	8.574
0.99	0.0311	8.2812	8.599

Table 5. Isotherm Data at 35 °C

t = 35 °C		P_o(35 °C) = 56.449 mbar	
adsorption			
P/mbar	P/P_0	q/mmol·g^{-1}	A/kJ·mol^{-1}
1.00	0.0177	6.2569	10.333
1.00	0.0177	6.1199	10.333
5.49	0.0973	8.7077	5.970
5.49	0.0973	8.6739	5.970
10.99	0.1947	9.7720	4.192
10.99	0.1947	9.7182	4.192
14.99	0.2655	10.3589	3.397
15.01	0.2659	10.4261	3.394
22.99	0.4073	11.7179	2.301
23.00	0.4074	11.8130	2.300
30.01	0.5316	13.2799	1.619
30.01	0.5316	13.1671	1.619
42.00	0.7440	16.5889	0.757
42.01	0.7442	16.9301	0.757
49.99	0.8856	25.8514	0.311
desorption			
P/mbar	P/P_0	q/mmol·g^{-1}	A/kJ·mol^{-1}
42.10	0.7458	17.8334	0.751
42.00	0.7440	18.3612	0.757
40.94	0.7253	17.8146	0.823
30.00	0.5315	14.8442	1.620
29.99	0.5313	14.5118	1.620
23.00	0.4074	12.9284	2.300
23.00	0.4074	13.0545	2.300
23.00	0.4074	12.8524	2.300
15.00	0.2657	11.1256	3.395
11.00	0.1949	10.5971	4.190
6.32	0.1120	9.8806	5.610
5.50	0.0974	9.5805	5.966
1.00	0.0177	7.1036	10.333

values). The more this value differs from 2, the greater the likelihood that the residuals are correlated, and the fit is not likely to describe the data well. The values of the D-W statistic in Table 8 are relatively close to the value of 2 for both adsorption and desorption.

The regressed DMAP parameters can be substituted in eq 1 to obtain adsorption and desorption isotherms at different temperatures. Figure 3 shows the fitted adsorption isotherms at (5 and 25) °C and compares them to the experimental data. It also shows the contributions of the individual terms in the DMAP equation. It is seen that the experimental data are very well represented by the DMAP equation. A comparison between experimental and fitted data at the other two temperatures (15 and 35 °C) exhibits the same trend and is not shown.

To gain insight into the mechanisms of water adsorption on CDX we look at the pore volumes of the adsorbent (Table 1) and the q-terms of the DMAP equation (Table 7). Computer simulation of adsorption in materials with both micropores and mesopores shows that adsorption first occurs within micropores.[20] These are the most energetically favorable sites, where water is expected to most strongly adsorb within the CDX. This has often been characterized as chemisorption.[2] Once the micropores are filled, the first layers of water are expected to form along the surface of the mesopores. The first layer of adsorbed water may be chemisorbed followed by several layers of physisorption. As we have stated earlier in the article, the term q_{s1} in the DMAP equation is meant to represent the molar loading that is a result of the combined effect of chemisorption and physisorption. The q_{s1} value of 13.9493 mmol·g^{-1} reported in Table 1 translates to a pore volume of 0.251 cm^3·g^{-1} which is consistent with the adsorption mechanism proposed above since it includes all of the estimated micropore volume (0.118 cm^3·g^{-1}) and a contribution of the mesopore volume as well, which may represent the first few layers of water molecules adsorbed along the surface of the mesopores. It can be seen from Figure 3 that up to 40 % relative humidity the total loading is exclusively due to

chemisorption and physisorption effects. Above 40 % relative humidity, capillary condensation within the mesopores appears to be the dominant mode of pore filling.

The heat of adsorption of water vapor on CDX as a function of fractional loading at 20 °C is presented in Figure 4. The fractional loading, θ, is defined as $\theta = q/q_{s2}$. Using the parameters from the fitted DMAP isotherms, we have compared the heat of adsorption calculated directly from the van't Hoff expression, eq 5, and from the simplified expression, eq 6, which assumes applicability of the Clausius−Clapeyron equation.

The term $-R_g(\partial \ln P/\partial(1/T))_q$ on the right-hand side of eq 5 is calculated from the slopes of the isosteres, $(\ln P)$ vs $(1/T)$ at constant loading, at (5, 15, 25, and 35) °C. The isosteres are constructed from the DMAP equation by varying T at constant q and solving for P. This method inherently assumes that the heat of adsorption does not vary within the given temperature range, that is, between (5 and 35) °C. The average temperature in this

Table 6. Experimental Uncertainty for Data with Three or More Replicate Measurements

t/°C	P/P_0	n	$\bar{q}$/mmol·g^{-1}	S/mmol·g^{-1}	δ/mmol·g^{-1}	$\delta/\bar{q}$
			adsorption			
5	0.0547	3	8.0076	0.0642	0.1595	0.0199
5	0.1723	3	9.3255	0.1586	0.3940	0.0423
5	0.3790	3	10.9711	0.1845	0.4584	0.0418
5	0.5732	3	13.0009	0.2125	0.5279	0.0406
5	0.6651	3	14.2034	0.1380	0.3429	0.0241
5	0.8615	3	17.4289	0.1691	0.4201	0.0241
15	0.0580	3	8.0829	0.0229	0.0568	0.0070
15	0.1171	4	8.8105	0.1647	0.2620	0.0297
15	0.3513	4	10.9843	0.1905	0.3031	0.0276
15	0.4684	4	12.2083	0.2229	0.3547	0.0291
15	0.7025	4	15.3503	0.1819	0.2894	0.0189
15	0.8782	4	18.9201	0.2365	0.3763	0.0199
			desorption			
5	0.6651	3	15.6274	0.2109	0.5239	0.0335
5	0.5743	5	14.4427	0.2705	0.3359	0.0233
35	0.4074	3	12.9451	0.1021	0.2536	0.0196

Table 7. DMAP Equation Parameters for Adsorption and Desorption of Water Vapor on Selexsorb-CDX in the Temperature Range between (5 and 35) °C

j	$q_{s,j}$ (std. error) mmol·g^{-1}	E_j (std. error) kJ·mol^{-1}
	Adsorption	
1	13.9493 (0.4956)	11.8619 (1.1431)
2	27.7093 (1.9022)	0.4209 (0.0780)
	Desorption	
1	14.3612 (0.5064)	14.2041 (1.3779)
2	27.7093 (2.1049)	0.6060 (0.1031)

Table 8. Statistics for the DMAP Equation Fits for the Adsorption and Desorption of Water Vapor on Selexsorb-CDX in the Temperature Range between (5 and 35) °C

	R^2	SEE	D-W
adsorption	0.9400	0.9744	1.7840
desorption	0.9722	0.5569	1.5851

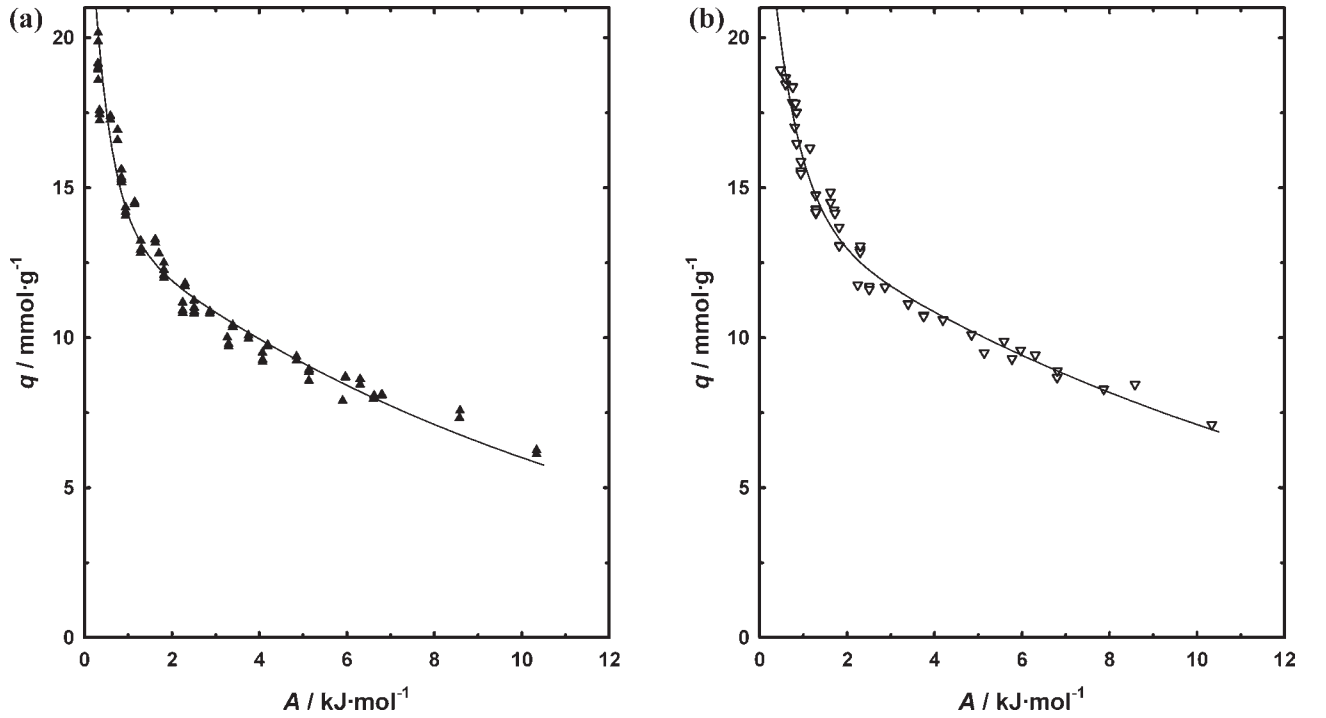

Figure 2. DMAP equation fits (—) to the experimental loadings, q, as a function of adsorption potential, A, for (a) adsorption (▲) and (b) desorption (▽) of water vapor on Selexsorb-CDX in the temperature range between (5 and 35) °C. All data are fitted with a single curve, yielding temperature independent adsorption isotherm parameters, shown in Table 7.

dx.doi.org/10.1021/je100473f |J. Chem. Eng. Data 2011, 56, 1762–1769

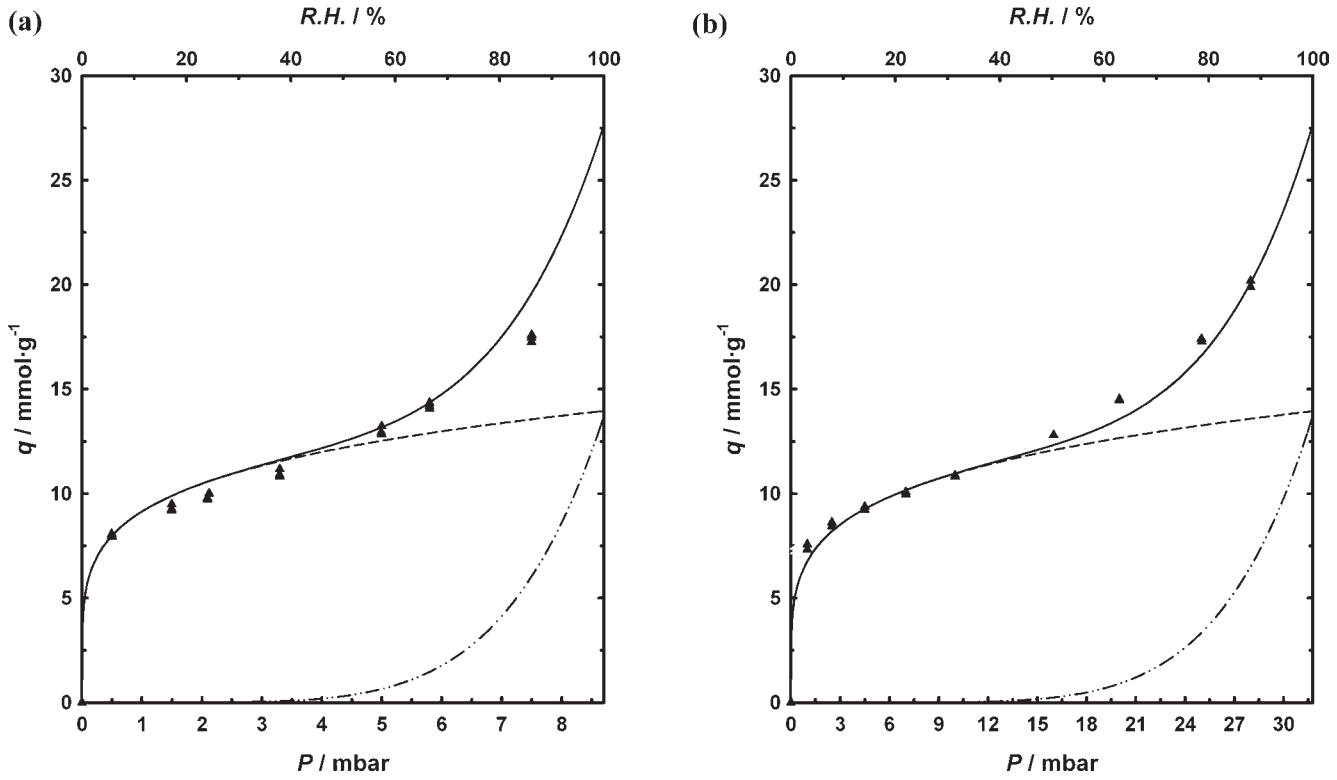

Figure 3. Comparison between the experimental data (▲) and the fitted DMAP equation (—) for water vapor adsorption on Selexsorb-CDX at (a) 5 °C and (b) 25 °C. The data are shown as a function of both pressure, *P*, and relative humidity (R.H.). (– – –) contribution of the first term in the DMAP equation accounting for chemisorbed and physisorbed water vapor; (– · · –) contribution of the second term in the DMAP equation accounting for capillary condensation.

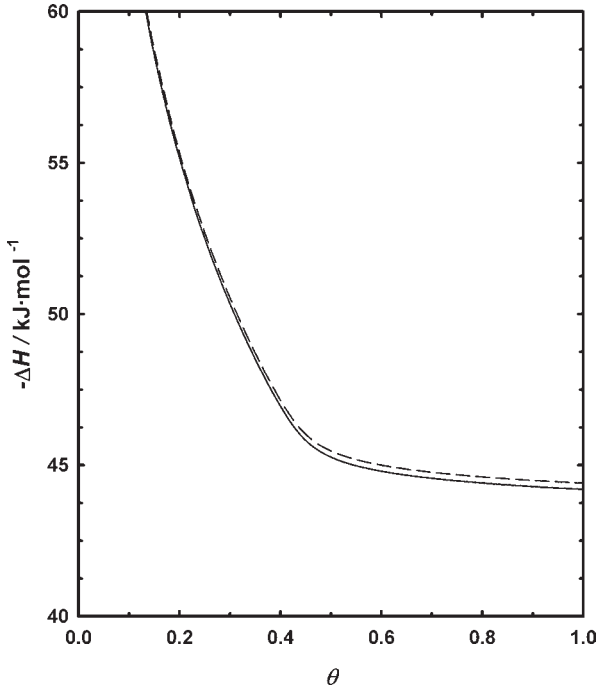

Figure 4. Heat of adsorption of water vapor, $-\Delta H$, at 20 °C as a function of fractional loading, θ, on Selexsorb-CDX, calculated from the DMAP model. (– – –) van't Hoff equation, eq 5; (—) van't Hoff equation assuming applicability of the Clausius–Clapeyron equation, eq 6.

range is 20 °C, and this is why in Figure 4 we present the heat of adsorption at 20 °C.

In Figure 4 we observe excellent agreement between the results obtained with and without the Clausius–Clapeyron assumption. This indicates that the Clausius–Clapeyron assumption is valid for water vapor in the range from (5 to 35) °C. The maximum difference is only 0.2 kJ·mol^{-1}. Thus, if one needs to calculate the heat of adsorption at other temperatures in the range between (5 and 35) °C, the simplified eq 6 can be used in place of the more complicated eq 5.

In the capillary condensation region, θ > 0.5, the heat of adsorption values calculated at 20 °C are very close to the heat of vaporization of water at 20 °C, 44.2 kJ·mol^{-1}, which is consistent with results reported in similar studies.[3] At zero coverage, the DMAP equation, like the Dubinin–Astakhov equation, does not predict the correct Henry's law behavior[9,10] and, thus, will not provide the correct heat of adsorption. This is why in Figure 4 we have not shown heat of adsorption results at fractional loadings close to zero.

CONCLUSIONS

The adsorption equilibrium of water vapor on Selexsorb-CDX, a commercially available activated alumina adsorbent, was measured at (5, 15, 25, and 35) °C in the relative humidity range between 0 % and 90 %. The experimental data were successfully correlated with the DMAP equation, which separates the contributions from different adsorption mechanisms. Pore size characterization studies using nitrogen adsorption indicated the presence of micropores in the material. From the best fit values of the DMAP parameters, we proposed that approximately 50 % of the adsorbed water was held by the combined effect of chemisorption and physisorption in the micropores and on the first adsorbed layers in the mesopores. The rest of the adsorbed

water was attributed to capillary condensation in the mesopores, the onset of which was observed around 40 % relative humidity. The heat of adsorption was calculated from the van't Hoff equation, with and without the assumption of the Clausius−Clapeyron equation. Both methods agreed, due to the validity of the Clausius−Clapeyron equation for water vapor between (5 and 35) °C. The calculated heats of adsorption for fractional loadings corresponding to capillary condensation were very close to the heat of vaporization.

AUTHOR INFORMATION

Corresponding Author

*Phone: +1 (812) 877-8097. Fax: (812) 877-8992. E-mail: serbezov@rose-hulman.edu.

Present Addresses

[†]U.S. Army Research Laboratory, Weapons and Materials Research Directorate, Aberdeen Proving Ground, Maryland 21005, United States.

[‡]Department of Chemical and Petroleum Engineering, University of Kansas, Lawrence, Kansas 66045, United States.

ACKNOWLEDGMENT

The authors wish to thank Mr. Riaz Ahmad at Quantachrome's Material Characterization Laboratory (LabQMC) for performing the material characterization measurements. The authors thank Jeremy C. Palmer, North Carolina State University, John K. Brennan, U.S. Army Research Laboratory, and Benoit Coasne, University of Montpellier, France, for helpful discussions.

REFERENCES

(1) Golden, T. C.; Kalbassi, M. A.; Taylor, F. W.; Allam, R. J. Use of zeolites and alumina in adsorption processes, U. S. Patent 5,779,767, July 14, 1998.

(2) Yang, R. T. *Adsorbents: Fundamentals and Applications*; Wiley: Hoboken, NJ, 2003.

(3) Desai, R.; Hussain, M.; Ruthven, D. M. Adsorption of Water Vapor on Activated Alumina. I - Equilibrium Behaviour. *Can. J. Chem. Eng.* **1992**, *70*, 699–706.

(4) Kotoh, K.; Enoeda, M.; Matsui, T.; Nishikawa, M. A. Multilayer Model for Adsorption of Water on Activated Alumina in Relation to Adsorption Potential. *J. Chem. Eng. Jpn.* **1993**, *26*, 355–360.

(5) Kim, J.-H.; Lee, C.-H.; Kim, W.-S.; Lee, J.-S.; Kim, J.-T.; Suh, J.-K.; Lee, J.-M. Adsorption Equilibria of Water Vapor on Alumina, Zeolite 13X, and a Zeolite X/Activated Carbon Composite. *J. Chem. Eng. Data* **2003**, *48*, 137–141.

(6) Serbezov, A. Adsorption Equilibrium of Water Vapor on F-200 Activated Alumina. *J. Chem. Eng. Data* **2003**, *48*, 421–425.

(7) Li, G.; Xiao, P.; Webley, P. Binary Adsorption Equilibrium of Carbon Dioxide and Water Vapor on Activated Alumina. *Langmuir* **2009**, *25*, 10666–10675.

(8) Ribeiro, A. M.; Sauer, T. P.; Grande, C. A.; Moreira, R. F. P. M.; Loureiro, J. M.; Rodrigues, A. E. Adsorption Equilibrium and Kinetics of Water Vapor on Different Adsorbents. *Ind. Eng. Chem. Res.* **2008**, *47*, 7019–7026.

(9) Moore, J. D.; Serbezov, A. Correlation of Adsorption Equilibrium Data for Water Vapor on F-200 Activated Alumina. *Adsorption* **2005**, *11*, 65–75.

(10) Do, D. D. *Adsorption Analysis: Equilibria and Kinetics*; Imperial College Press: London, 1998.

(11) Shen, D.; Bülow, M.; Siperstein, F.; Engelhard, M.; Myers, A. L. Comparison of Experimental Techniques for Measuring Isosteric Heat of Adsorption. *Adsorption* **2000**, *6*, 275–286.

(12) Sandler, S. I. *Chemical and Engineering Thermodynamics*, 3rd ed.; Wiley: New York, 1999.

(13) Sing, K. S. W.; Everett, D. H.; Haul, R. A. W.; Moscou, L.; Pierotti, R. A.; Rouquerol, J.; Siemieniewska, T. Reporting Physisorption Data for Gas/Solid Systems with Special Reference to the Determination of Surface Area and Porosity. *Pure Appl. Chem.* **1985**, *57*, 603–619.

(14) de Boer, J. H.; Lippens, B. C.; Linsen, B. G.; Broekhoff, J. C. P.; van den Heuval, A.; Osinga, Th. J. The t-curve of Multimolecular N_2-adsorption. *J. Colloid Interface Sci.* **1966**, *21*, 405–414.

(15) Gregg, S. J.; Sing, K. S. W. *Adsorption, Surface Area and Porosity*, 2nd ed.; Academic Press: London, 1982.

(16) Brunauer, S.; Emmett, P. H.; Teller, E. Adsorption of Gases in Multimolecular Layers. *J. Am. Chem. Soc.* **1938**, *60*, 309–319.

(17) Walton, K. S.; Snurr, R. Q. Applicability of the BET Method for Determining Surface Areas of Microporous Metal-Organic Frameworks. *J. Am. Chem. Soc.* **2007**, *129*, 8552–8556.

(18) Wheeler, A.; Ganji, A. *Introduction to Engineering Experimentation*; Prentice-Hall: Upper Saddle River, NJ, 2004.

(19) *SigmaPlot*, version 7.0; Systat Software, Inc.: Point Richmond, CA, 2001.

(20) Bhattacharya, S.; Coasne, B.; Hung, F. R.; Gubbins, K. E. Modeling Micelle-Templated Mesoporous Material SBA-15: Atomistic Model and Gas Adsorption Studies. *Langmuir* **2009**, *25*, 5802–5813.